# Study on the relationship between process organization and properties of 45MnVS non-tempered steel

Xu Yuan[1] , Xin-Qing Yan[1], Jun-Ru Li[1], Zong-Qiang Liu[2]

[1]Qingdao University, College of Mechanical and Electrical Engineering. 266071, Qingdao, China.

[2]QING TE Group Co., Ltd. 266109, Qingdao, China

e-mail: lijunru_qdu@163.com, 17853266382@163.com, LJR17806240085@163.com, 1538638097@qq.com

## ABSTRACT

The microstructure, mechanical properties, and heat treatment process relationships of 45MnVS non-tempered steel were investigated. Different grain sizes and tissue ratios were obtained after heating and holding at 950, 1050, and 1150 °C for 30 min, respectively, and cooling at different cooling conditions and cooling rates. As the austenitizing temperature increased, the grain size and the elongation and section shrinkage of the experimental steels decreased. At the same time, the content of ferrite and pearlite in the tissue gradually decreases, the content of sorbite and troostite rises, and the strength and hardness of the experimental steel increase. With the increase of cold speed, ferrite's content decreases, sorbite and troostite's content increases, and strength and hardness increase. The original austenite grain size also influences the tissue ratio. As the austenite grain refines, the ferrite transformation temperature increases during cooling and the ferrite content in the tissue rises after cooling.

**Keywords:** 45MnVS steel; Heat Treatment; Organizational ratio; Mechanical properties.

## 1. INTRODUCTION

Non-tempered steel refers to a new type of steel formed by adding trace amounts of vanadium, niobium, titanium, and other alloying elements to traditional steel, which eliminates the need for "tempered treatment" of parts and can reduce costs and energy consumption [1, 2]. The machined parts have the characteristics of high precision and small size effect. They can avoid the problems of quenching deformation and cracking of long-axis parts, which is conducive to improving the quality of products. Therefore, researchers in the automotive industry at home and abroad are committed to applying non-tempered steel in automotive forgings [3–9].

As a type of high-quality steel with high strength and toughness, non-tempered steel can effectively improve the bearing capacity of the axle and is more and more widely used in automobile axles. Ferritic and pearlescent type non-quenched steel is an early development of non-quenched steel [10, 11], 45MnVS is a type of sulfur-free cutting non-tempered steel, the matrix structure is ferritic, perlite, sorbite, and troostite, mainly used in the production of automobile connecting rods, crankshaft, and other shaft parts [12–14].

This paper mainly studies the relationship between the microstructure and properties of 45MnVS non-tempered steel and studies the relationship between microstructure (ferrite and pearlite) ratio and properties of experimental steel under different heating temperatures and different cooling conditions, which lays a foundation for the optimization of the hot working process of 45MnVS non-tempered steel and the application of 45MnVS non-tempered steel in automobile shaft manufacturing.

## 2. MATERIALS AND METHODS

The research object of this subject is a 45MnVS non-tempered steel, the chemical composition is shown in Table 1, the original microstructure of the experimental steel (normalizing state) is shown in Figure 1, the original microstructure of the experimental steel is ferrite, and the pearlite. The white strip structure is ferrite, the tissue with obvious lamellar structure is pearlite, and the dark part is sorbite or troostite.

The experimental steel specimens (12 mm × 12 mm × 70 mm) were prepared by using wire-cutting machine tools, and the corresponding heat treatment experiments were carried out in an SX-G04133 chamber muffle furnace. The specimens were heated at 950, 1050, and 1150 °C and held for 30 min to obtain different

pearlite cluster sizes, then the specimens were removed and immediately cooled in a low-temperature furnace preheated to 550 °C to study the influence of pearlite cluster size on mechanical properties; The other group of specimens were heated at 1050 °C for 30 min and then cooled in the low-temperature furnace at 610, 580, 550 and 520 °C to obtain different microstructure ratios and study the effect of microstructure ratio on mechanical properties.

The specimens after heat treatment were subjected to the use of microscopes and mechanical property testing, including hardness and tensile mechanical property testing. The samples were corroded with 4% (volume fraction) nitrate alcohol solution at different heating temperatures and the microstructure was observed with a ZEISS Axioscope 5 optical microscope. Before the tensile mechanical property test, the specimens were processed into standard tensile specimens of diameter $\phi 5$ mm according to GB/T228.1-2021 national standard, and the tensile test was performed on the universal testing machine WDW-100, as shown in Figure 2. Image Tool software was used to calculate the content and proportion of each microstructure.

**Table 1:** Composition analysis of experimental steels (mass fraction,%).

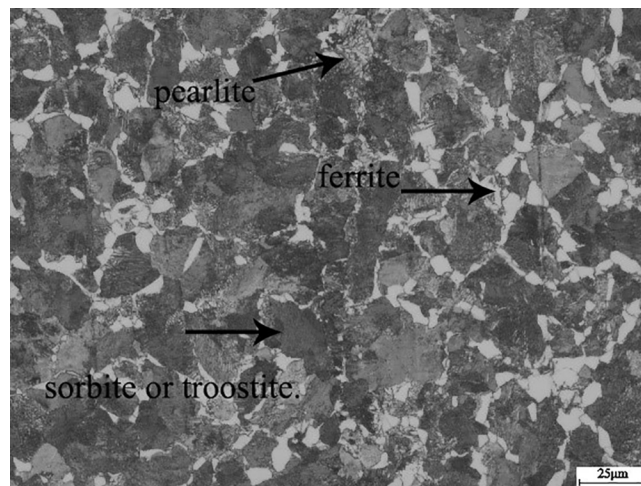| C | Si | Mn | P | S | Ni | Cr | Mo | Ti | V | Fe |
|---|---|---|---|---|---|---|---|---|---|---|
| 0.47 | 0.43 | 1.41 | 0.013 | 0.047 | 0.007 | 0.18 | 0.002 | 0.02 | 0.089 | Bal |



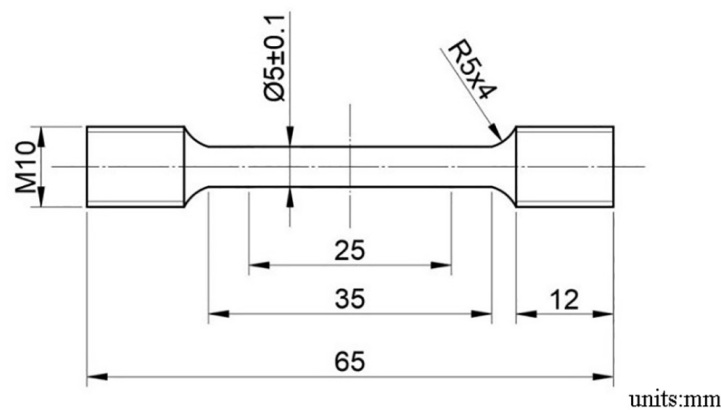**Figure 1:** Original microstructure of experimental steel.



**Figure 2:** Diagram of tensile specimen.

## 3. RESULTS

### 3.1. Effect of heating temperature on tissue properties

The cooling curves of the samples after heating and holding at 950, 1050, and 1150 °C for 30 min are shown in Figure 3. With the onset of cooling, the temperature drops sharply, and the rate of temperature drop gradually slows down as the cooling time is prolonged. The temperature increases with time at about 610 °C, which may be due to the transition temperature of pearlite. The phase transition temperature Ac3 of the experimental steel is about 775 °C, and the cooling rate is calculated only in the range of 775~630 °C when the cooling rate is relatively stable before the phase transition heating. The cooling rate at 950, 1050, and 1150 °C is 1.74, 1.21, and 0.85 °C/s, respectively, which indicates that the cooling rate gradually decreases with the increase of austenitizing temperature in the range of 775~630 °C.

The microstructures of the specimens after heating at 950, 1050, and 1150 °C for 30 min are shown in Figure 4. The cooled section of the specimens after heating at different austenitizing temperatures all consisted of ferrite and pearlite (including pearlite, siderite, and troostite). Still, the ferrite size and pearlite pellet size in the cooled tissues increased significantly with the increase of austenitizing temperature, which indicated that the austenitizing temperature had a significant effect on the size of ferrite and pearlite. After cooling at different austenitizing temperatures, the microstructure ratios were counted, and the results are shown in Figure 5 [15]. From the statistical results, it can be seen that the content of ferrite and pearlite in the cooled specimens gradually decreases as the austenitizing temperature increases.

The mechanical properties of the sample after heating and cooling at different austenitizing temperatures are shown in Figure 6. The mechanical properties test results show that the tensile properties of the samples heated at three austenitizing temperatures meet the requirements of GB/T 15712-2016 standard (tensile strength Rm ≥ 810 MPa, lower yield strength ReL ≥ 490 MPa, post-fracture elongation A ≥ 12%, section shrinkage Z≥ 28%). With the increase of austenitizing temperature, the strength and hardness of the material increase, the elongation and section shrinkage decrease, and the mechanical properties of the material decrease gradually with the increase of austenitizing temperature. This indicates that the strength of the experimental steel can be improved by increasing the austenitizing temperature, but the mechanical properties change from 1050 °C to 1150 °C is significantly less than that from 950 °C to 1050 °C.

The fracture morphology of the tensile sample was observed, as shown in Figure 7. As can be seen from the figure, the tensile sample mainly fractures in the form of dimples, which are randomly distributed on the fracture surface of the sample. The dimples in the fracture of the sample at 950 °C and 1050 °C are small and have a certain depth, indicating that the sample has good plasticity, as shown in Figure 7(a,b). However, after heating at 1150 °C, in addition to the small and deep dimples in the fracture of the sample, there are also some shallow dimples or pits with smooth edges, as shown in Figure 7(c), indicating poor plasticity of the sample at 1150 °C. The tensile fracture morphology of mechanical properties shows that the plasticity of the experimental steel decreases obviously with the increase of austenitizing temperature and pearlite group [16].
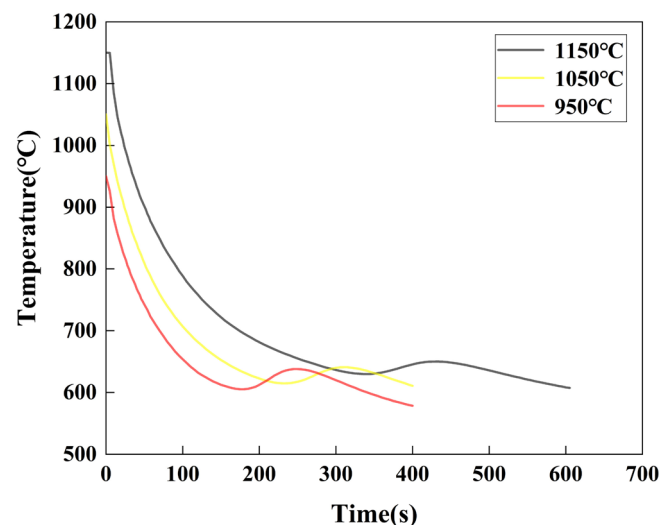


**Figure 3:** Cooling curves of the specimens after different austenitizing temperatures.
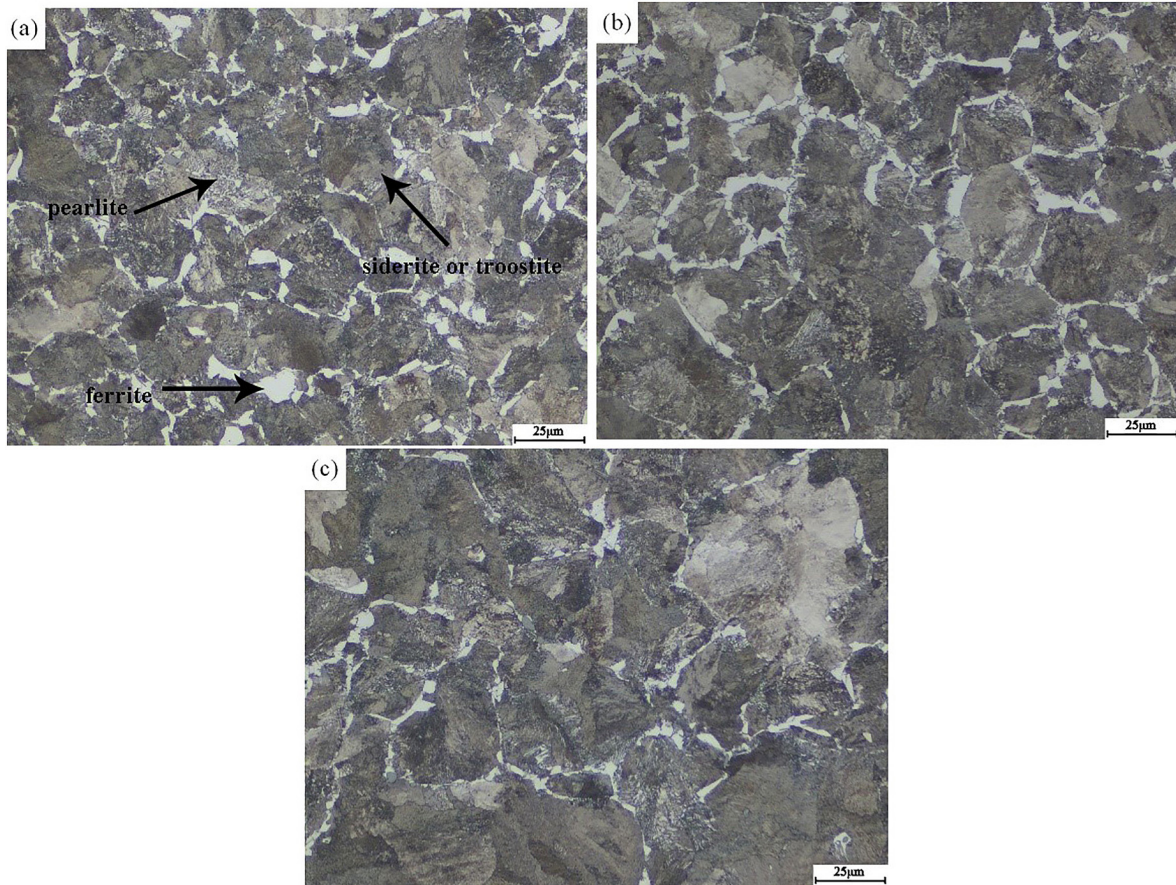
**Figure 4:** Microstructure of samples heated at different austenitizing temperatures (a) 950 °C; (b) 1050 °C; (c) 1150 °C.
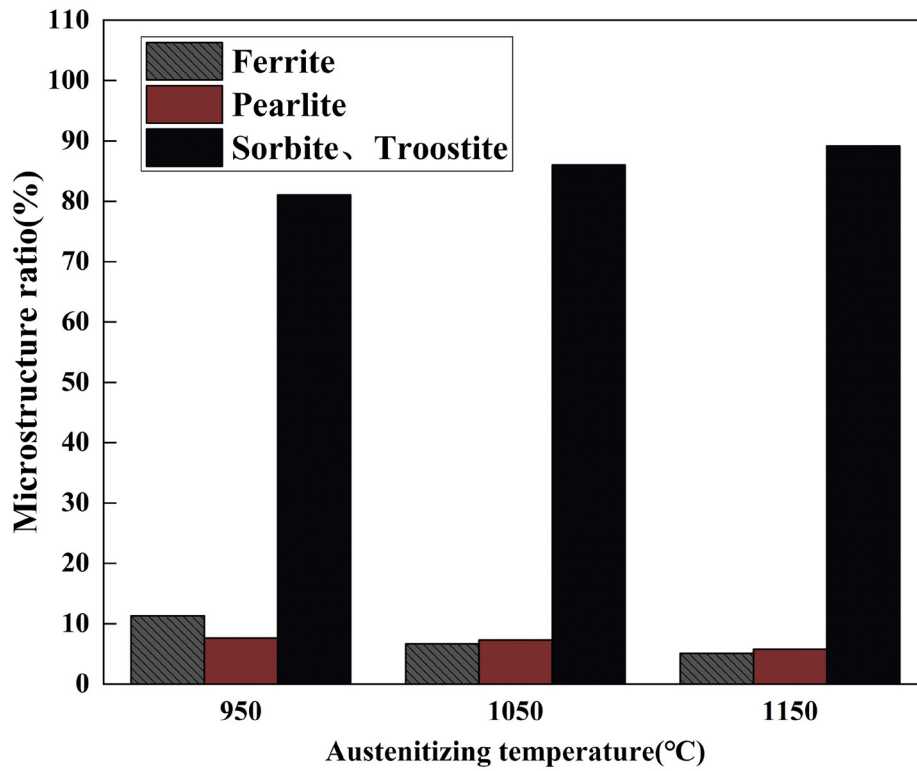


**Figure 5:** Microstructure percentage of the specimens after austenitizing at different temperatures.
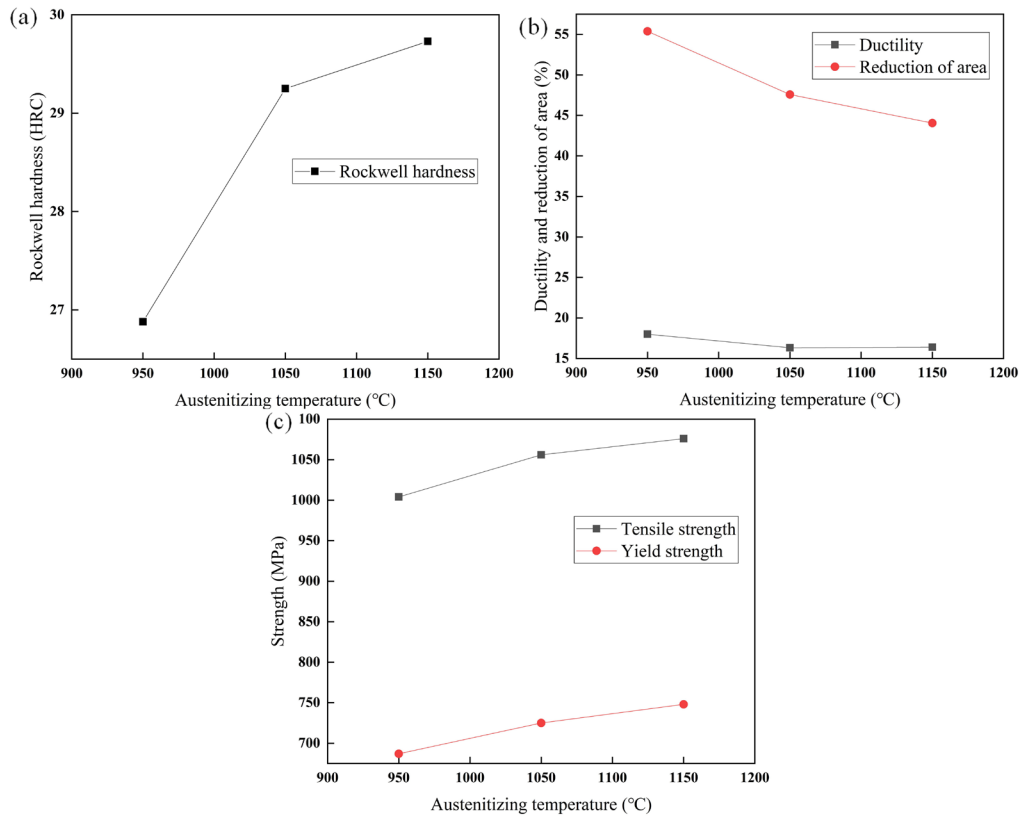
**Figure 6:** Mechanical properties of the specimens after austenitizing at different temperatures (a) rockwell hardness; (b) ductility and reduction of the area; (c) strength.
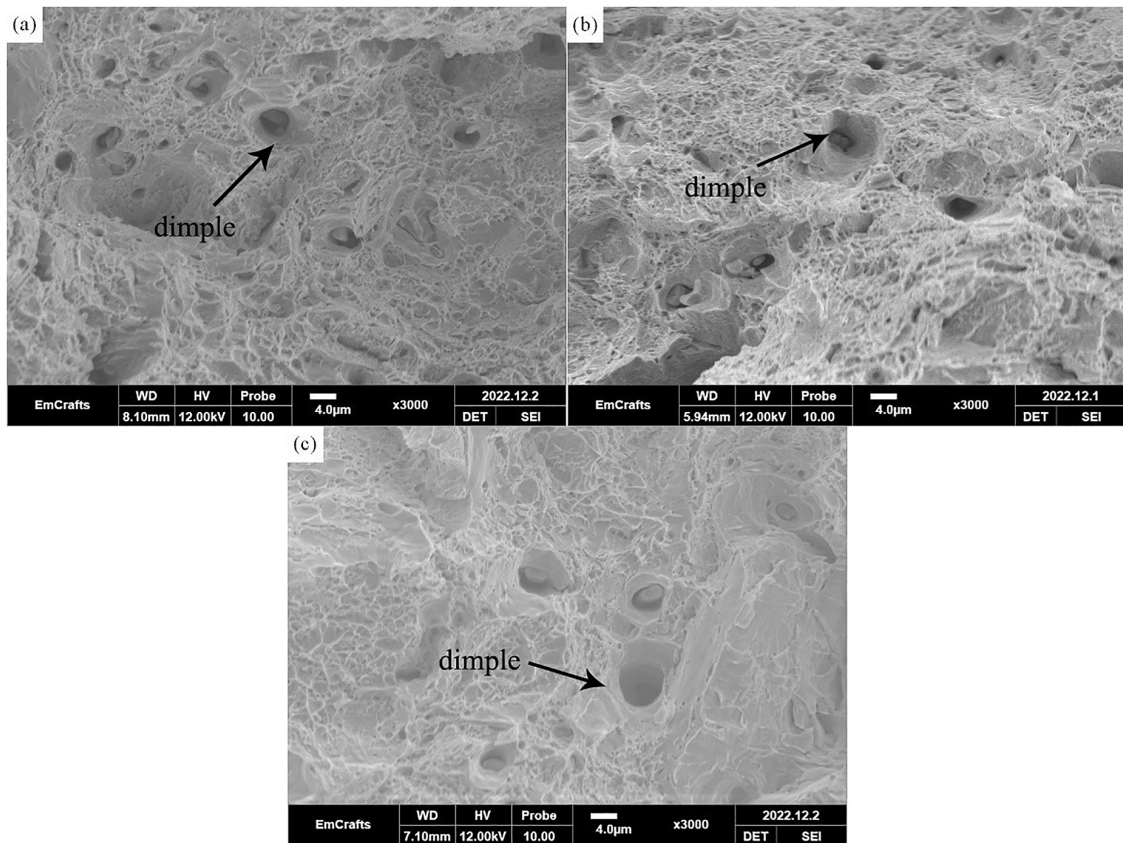


**Figure 7:** Fracture morphology of tensile specimens heated at different austenitizing temperatures (a) 950 °C; (b) 1050 °C; (c) 1150 °C.
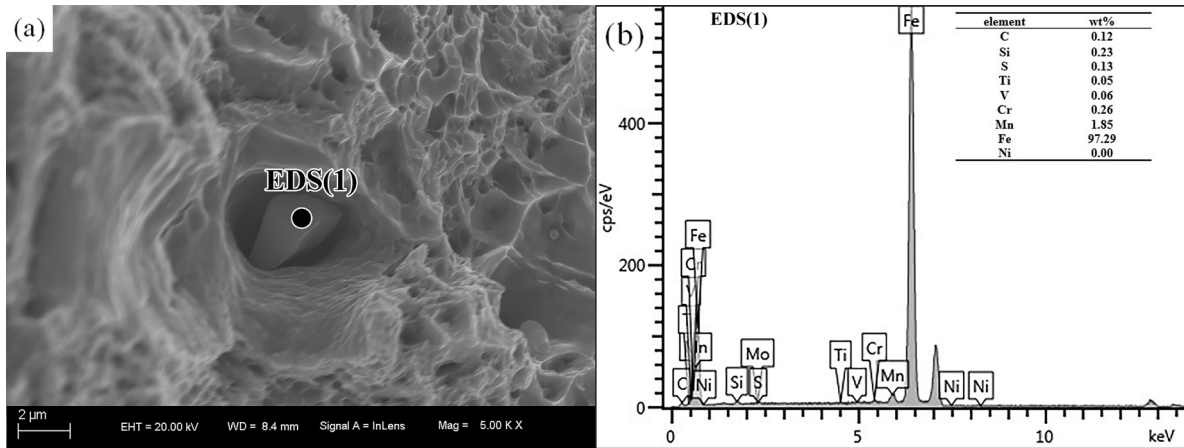
**Figure 8:** EDS analysis of particles at the bottom of dimples.
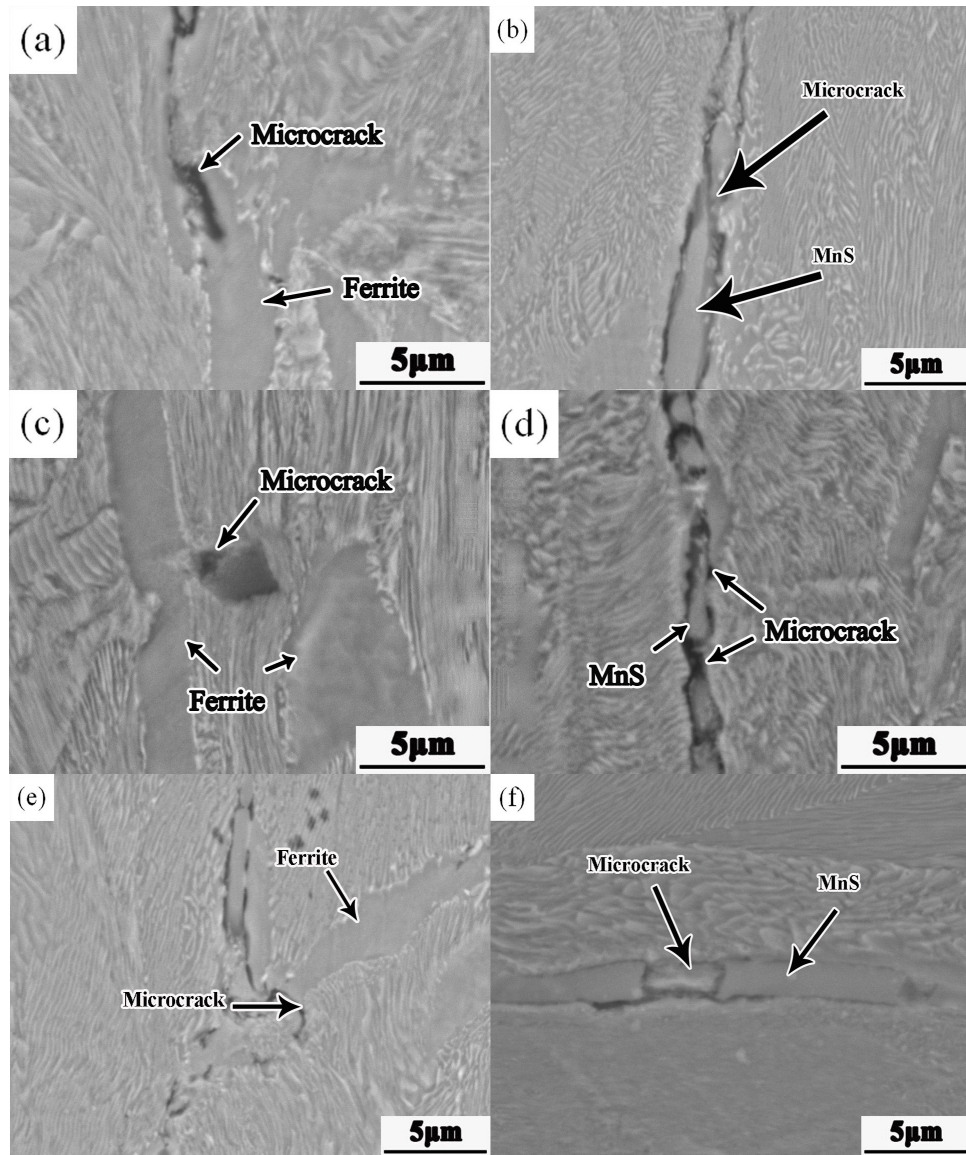


**Figure 9:** Microstructure near fracture of tensile specimens heated at different austenitizing temperatures (a)(b) 950 °C; (c)(d) 1050 °C; (e)(f) 1150 °C.

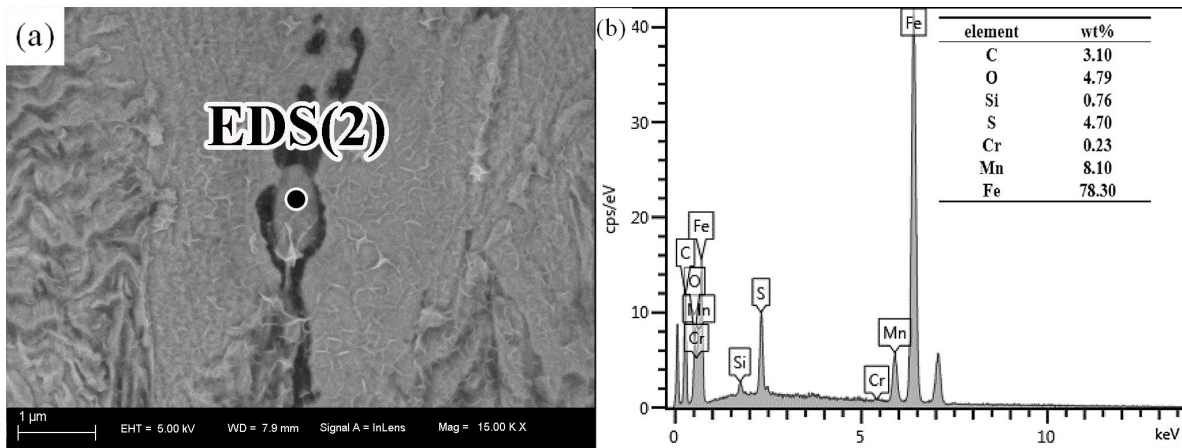| element | wt% |
|---------|-------|
| C | 3.10 |
| O | 4.79 |
| Si | 0.76 |
| S | 4.70 |
| Cr | 0.23 |
| Mn | 8.10 |
| Fe | 78.30 |

**Figure 10:** EDS analysis of precipitated phase near microcracks.

In addition, in the observation of the fracture morphology of tensile specimens, it is found that some of the dimpled particles are different from the matrix, and such particles exist in the samples at different austenitizing temperatures. To determine the composition of the particles, EDS analysis was performed on the particles at the bottom of the dimples. The calibration location of EDS and the analysis results are shown in Figure 8. According to the EDS results, the content of Mn and S elements in the particles was much higher than that in the matrix.

To further analyze the relationship between the microstructure, fracture, and mechanical properties of the experimental steel, the tensile fracture of the experimental steel was cut lengthwise to observe the micro-cracks near the fracture, as shown in Figure 9. From the figure, it can be seen that microcracks mainly appear near the ferrite and MnS precipitation phases.

EDS analysis was performed on the precipitated phase near the microcrack, and the results are shown in Figure 10.

## 3.2. Effect of cooling rate on tissue properties

Through the study on the tissue properties of ferrite-pearlite type non-tempered steel, it is found that the microstructure ratio also has a significant impact on its properties: increasing the ferrite content can improve the plasticity of ferrite-pearlite type non-tempered steel, and its strength and toughness mainly depend on the pearlite lamellar spacing, the smaller the lamellar spacing, the higher the content of sorbite and troostite, the better the strength and toughness of steel. The cooling rate is the key factor affecting the microstructure ratio of steel after cooling. The relationship between microstructure ratio and mechanical properties was studied by designing different cooling rate experiments and obtaining different microstructure ratios.

After the sample is heated at 1050 °C for 30 min, the cooling curves at different cooling rates are shown in Figure 11. Cooling rate-1, cooling rate-2, cooling rate-3, and cooling rate-4 indicate that the sample is cooled in the heating furnace at 610, 580, 550, and 520 °C, respectively. The cooling rate in the range of 775~630 °C, where the cooling rate is relatively stable, is calculated. The cooling rates of Rate-1, rate-2, rate-3, and rate-4 are 0.62, 0.88, 1.21, and 1.65 °C/s, respectively.

The microstructure of samples at different cooling rates is shown in Figure 12. With the increase in cooling rate, the contents of ferrite and pearlite in the tissues decreased significantly, and the ferrite decreased from 11.55% when the furnace was cooled at 610 °C (0.62 °C/s) to 6.06%when the furnace was cooled at 520 °C (1.65 °C/s), while the pearlite content decreased from 13.53% to 2.85%, as shown in Figure 13 [17].

The mechanical properties of the samples at different cooling rates are shown in Figure 14. As the cooling rate increases, the strength and hardness of the materials increase significantly, the elongation decreases, and the section shrinkage does not change significantly. Compared with austenitizing temperature, the cooling rate less affects ductility and toughness.
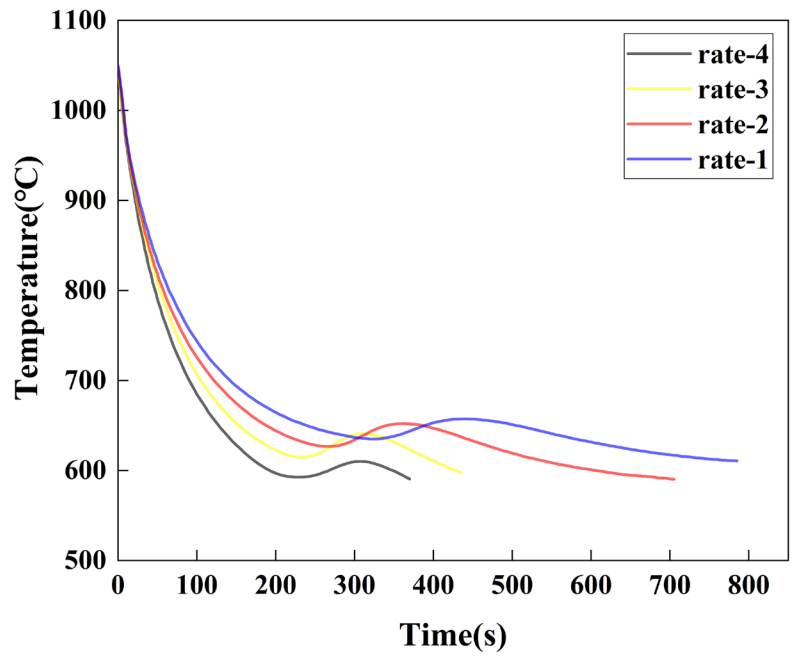
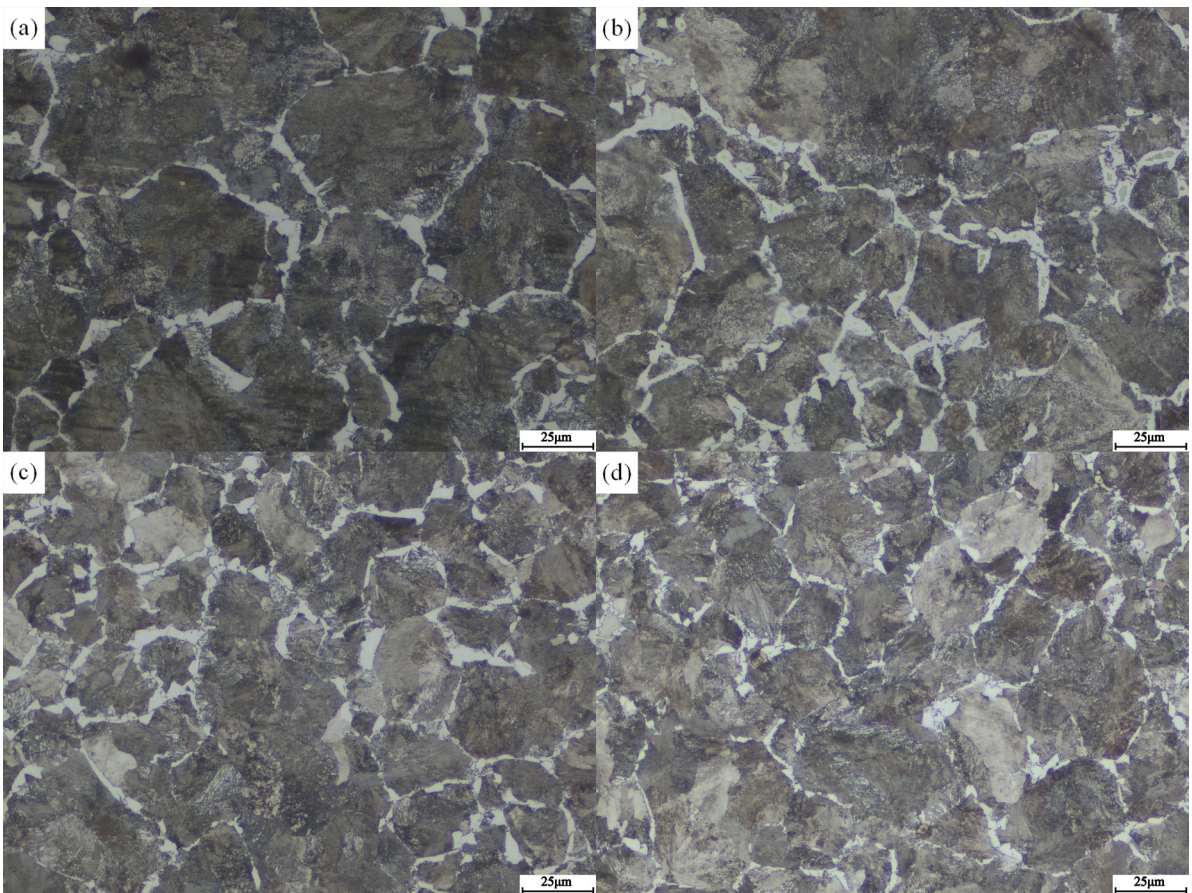**Figure 11:** Cooling curves of the specimens after austenitizing with different cooling rates.



**Figure 12:** Microstructure of samples cooled at different cooling rates (a) rate-1; (b) rate-2; (c) rate-3; (d) rate-4.
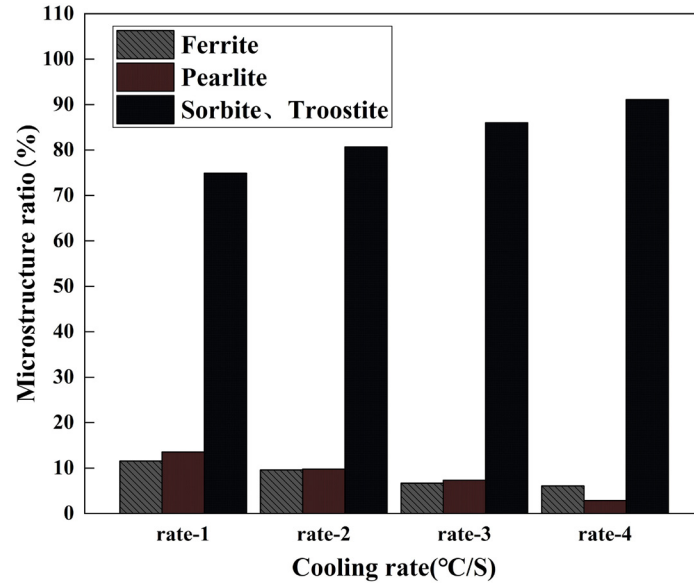
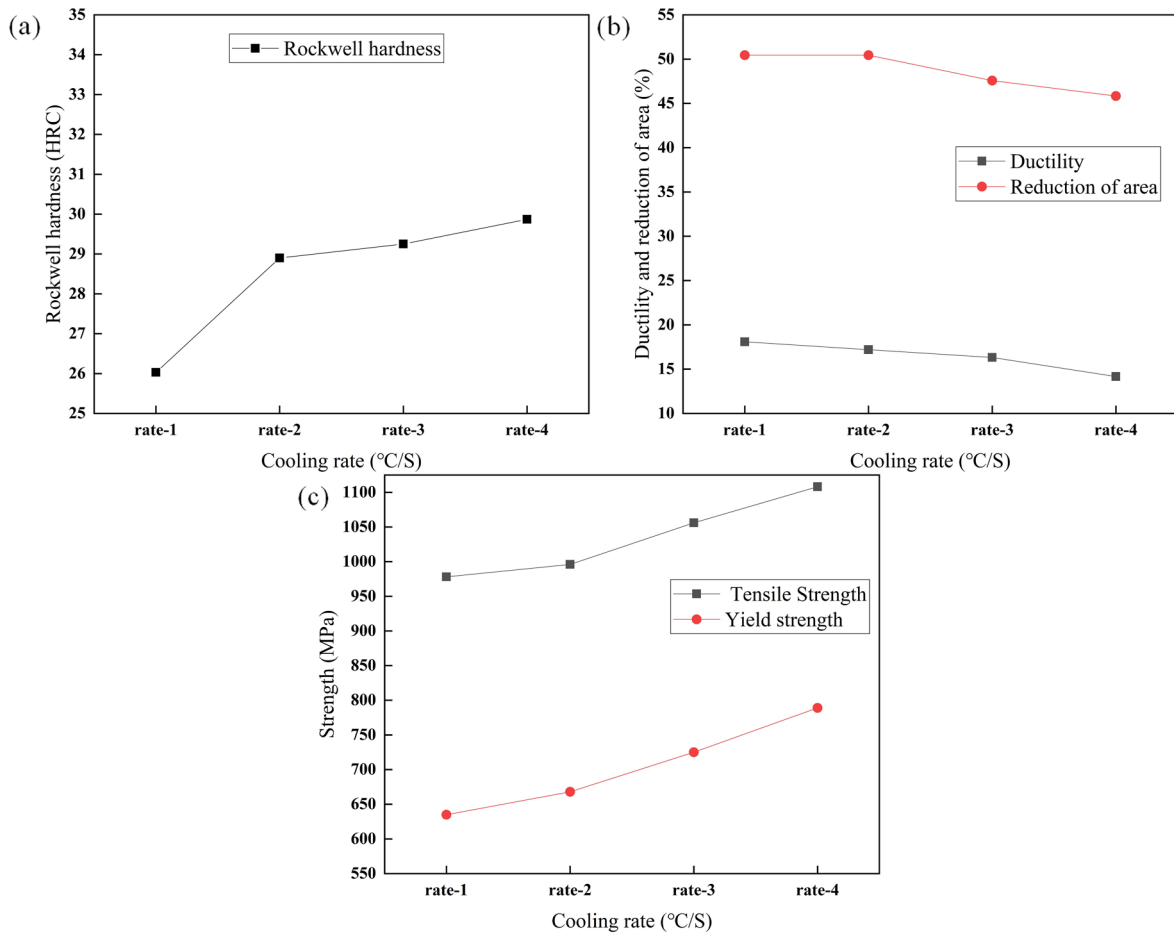**Figure 13:** Microstructure percentage of the specimens after cooling with different rates.



**Figure 14:** Mechanical properties of the specimens after cooling with different rates (a) rockwell hardness; (b) ductility and reduction of the area; (c) strength.

## 4. DISCUSSION

The above results show that for 45MnVS, the microstructure ratio is the main factor affecting its strength and hardness, and the microstructure ratio is mainly affected by the cooling rate. With the increase of cooling rate, the content of ferrite and pearlite decreases, sorbite and troostite increase, the strength and hardness of the experimental steel increase, and the plasticity deteriorates . With the increase of austenitizing temperature, the original austenite grains grow, the corresponding pearlite group size also increases, the strength and hardness of the experimental steel increase, and the elongation and section shrinkage decrease [18, 19].

According to the observation of the fracture of different samples, the micro-cracks near the fracture of the samples are mainly generated in two positions: First, the junction of ferrite and pearlite, where ferrite has good plasticity and low hardness, and pearlite laminate has high hardness. Due to the difference in mechanical properties of ferrite and pearlite, microcracks appear at the junction of the two during the stretching process. Second, near the precipitated phase, there is also a difference in mechanical properties between the precipitated phase and the matrix, and it is easy to produce stress concentration near the precipitated phase, leading to the generation of microcracks. The content of S and Mn elements precipitated along with the substrate is significantly higher than that of the matrix [7, 20]. A comprehensive analysis of the microstructure, fracture, and microcrack shows that the particles at the bottom of the dimple are MnS precipitated phase. The MnS precipitates in the experimental steel promote the generation of microcracks and affect the mechanical properties of the experimental steel [21, 22].

There is a significant effect of cooling rate on the microstructure ratio and mechanical properties of 45MnVS steel, which is because as the cooling rate increases, the greater the subcooling in the cooling process, which leads to a lower pearlite phase transformation temperature, an increase in the content of sorbite and troostite, and an increase in the strength and hardness of the experimental steel. On the other hand, with the increase of cooling rate, the pearlescent layer spacing decreases, so the plastic change of the experimental steel is small, so the tensile property of the experimental steel can be improved by increasing the cooling rate [23].

With the increase of austenitizing temperature, the pearlite group increases, and after cooling under the same cooling conditions, the content of ferrite and pearlite decreases, the content of sorbite and troostite increases, and the strength and hardness of the experimental steel increase. Elongation and section shrinkage decreased. The higher the austenitizing temperature, the larger the grain size. Generally, the larger the grain size of austenite will increase the stability of austenite to a certain extent [16, 24], reducing the pearlite phase transition temperature. At the same time, reducing grain boundaries will reduce the ferritic core point during the cooling process, which can inhibit the formation of ferrites. The content of pearlite and ferrite decreased, the content of sorbite and troostite increased, the strength and hardness of the experimental steel increased, and the plasticity decreased.

To sum up, it can be seen that the original austenite grain state and cooling rate should be comprehensively considered, based on increasing the cooling rate, increasing the content of sorbite and troostite, and reducing the grain size to ensure that the experimental steel has enough plasticity and toughness, to obtain the experimental material with good comprehensive mechanical properties.

## 5. CONCLUSIONS

(1) The grain size is related to the austenitizing temperature. With the austenitizing temperature increasing, the grain size increases, the elongation and section shrinkage decrease, and the plasticity deteriorates. At the same time, with the increase of austenitizing temperature, the content of ferrite and pearlite decreased, the content of sorbite and troostite increased, and the strength and hardness of the experimental steel increased.

(2) The grain size is related to the austenitizing temperature. With the austenitizing temperature increasing, the grain size increases, the elongation and section shrinkage decrease, and the plasticity deteriorates. With the increase of austenitizing temperature, the content of ferrite and pearlite decreased, the content of sorbite and troostite increased, and the strength and hardness of the experimental steel increased.

## 6. ACKNOWLEDGMENTS

## 7. BIBLIOGRAPHY

[1] MAN, T.H., GAO, P., HE, Y.G., *et al*., "Effect of forging process on V-Nb-Ti microalloyed non-quenched and tempered steels", *Advanced Materials Research*, v. 936, pp. 1179–1183, 2014. doi: http://dx.doi.org/10.4028/www.scientific.net/AMR.936.1179.

[2] WANG, Q., SHI, J., CAI, J., *et al*., "Deformation behavior and processing map during isothermal hot compression of 49MnVS3 non-quenched and tempered steel", *High-Temperature Materials and Processes*, v. 38, n. 2019, pp. 452–460, 2019. doi: http://dx.doi.org/10.1515/htmp-2018-0042.

[3] BO, Z., YONG, S., LI, T., *et al*., "Research on a new process of the non-quenched and tempered steel with high strength and high toughness", *Physics Procedia*, v. 50, pp. 25–31, 2013. doi: http://dx.doi.org/10.1016/j.phpro.2013.11.006.

[4] LI, X., LI, X.X., LI, M.Y., *et al*., "Friction correction and constitutive equation of a non-quenched and tempered steel during hot deformation", *Advanced Materials Research*, v. 634, pp. 2843–2848, 2013. doi: http://dx.doi.org/10.4028/www.scientific.net/AMR.634-638.2843.

[5] WANG, T.T., YANG, S.F., LI, J.S., *et al*., "Effect of in situ observation of cooling rates on acicular ferrite nucleation", *High-Temperature Materials and Processes*, v. 41, n. 1, pp. 181–190, Apr. 2022. doi: http://dx.doi.org/10.1515/htmp-2022-0026.

[6] LIU, P., LIU, R., WEI, Y., *et al*., "Austenite dynamic recrystallization of the microalloyed forging steels 38MnVS during forging process", *Procedia Engineering*, v. 27, pp. 63–71, 2012. doi: http://dx.doi.org/10.1016/j.proeng.2011.12.425.

[7] LI, M.L., WANG, F.M., LI, C.R., *et al*., "Effects of cooling rate and Al on MnS formation in medium-carbon non-quenched and tempered steels", *International Journal of Minerals Metallurgy and Materials*, v. 22, n. 6, pp. 589–597, Jun. 2015. doi: http://dx.doi.org/10.1007/s12613-015-1111-1.

[8] LIU, H., HUANG, Z.Z., YU, D.J., *et al*., "Effect of cooling rate on microstructure and inclusion in non-quenched and tempered steel during horizontal directional solidification", *Journal of Iron and Steel Research International*, v. 26, n. 9, pp. 10, Sep. 2019. doi: http://dx.doi.org/10.1007/s42243-019-00282-2.

[9] LIU, J.Y., LIU, C.S., BAI, R.J., *et al*., "Morphological transformation of elongated MnS inclusions in non-quenched and tempered steel during isothermal heating", *Journal of Iron and Steel Research International*, v. 30, n. 3, pp. 525–536, Mar. 2022. doi: http://dx.doi.org/10.1007/s42243-022-00829-w.

[10] WANG, K., YU, T., SONG, Y., *et al*., "Effects of MnS inclusions on the banded microstructure in non-quenched and tempered steel", *Metallurgical and Materials Transactions. B, Process Metallurgy and Materials Processing Science*, v. 50, n. 3, pp. 1213–1224, Jun. 2019. doi: http://dx.doi.org/10.1007/s11663-019-01532-0.

[11] CHEN, Y.F., PENG, X.D., XU, H.B., *et al*., "Constitutive equations and processing maps for 49MnVS3 non-quenched and tempered steel", *Strength of Materials*, v. 46, n. 2, pp. 198–207, Mar. 2014. doi: http://dx.doi.org/10.1007/s11223-014-9536-8.

[12] XIAO, B., PARK, Y.C., SU, H.H., *et al*., "The influence of grinding parameters on the superficial hardening effect of 48MnV microalloyed steel", *Key Engineering Materials*, v. 315, pp. 15–19, 2006. doi: http://dx.doi.org/10.4028/www.scientific.net/KEM.315-316.15.

[13] LIU, J., PENG, T., TIAN, Z., *et al*., "Effect of cooling rate and Nb on the microstructure and hardness variation in microalloying medium-carbon non-quenched and tempered steel simulated in a die forging process", *Journal of Materials Engineering and Performance*, v. 31, n. 8, pp. 6561–6571, Aug. 2022. doi: http://dx.doi.org/10.1007/s11665-022-06733-4.

[14] PEITSCH, P.E.R., DANÓN, C.A., "Study of the behavior of the reduced activation martensitic ferritic steel F82H under continuous cooling", *Matéria (Rio de Janeiro)*, v. 23, n. 2, pp. 13, 2018.

[15] KHAJURIA, A., AKHTAR, M., BEDI, R., "Boron addition to AISI A213/P91 steel: preliminary investigation on microstructural evolution and microhardness at simulated heat-affected zone", *Materialwissenschaft und Werkstofftechnik*, v. 53, n. 10, pp. 1167–1183, 2022. doi: http://dx.doi.org/10.1002/mawe.202100152.

[16] LI, J.R., SUN, X.H., JI, Y., *et al*., "Effects of austenitizing temperature and cooling rate on the mechanical properties of 36MnVS4 steel for automobile engine connecting rod", *Materials Science Forum*, v. 898, n. 2, pp. 1195–1201, Jun. 2017. doi: http://dx.doi.org/10.4028/www.scientific.net/MSF.898.1195.

[17] AKHTAR, M., KHAJURIA, A., SAHU, J.K., *et al*., "Phase transformations and numerical modelling in simulated HAZ of nanostructured P91B steel for high temperature applications", *Applied Nanoscience*, v. 8, n. 7, pp. 1669–1685, 2018. doi: http://dx.doi.org/10.1007/s13204-018-0854-1.

[18] GUIQIN, F., DUO, J., MIAOYONG, Z., "Effect of austenitizing temperature on the microstructure and mechanical properties of Nb - Ti microalloyed steel", *Journal of Engineering Science and Technology Review*, v. 8, n. 4, pp. 43–50, Oct. 2015. doi: http://dx.doi.org/10.25103/jestr.084.07.

[19] WU, G.H., WU, K.M., ISAYEV, O., *et al*., "Effect of austenitizing temperature on pearlite transformation of a medium-carbon steel", *Metallurgist*, v. 62, n. 9–10, pp. 1073–1080, Jan. 2019. doi: http://dx.doi.org/10.1007/s11015-019-00756-4.

[20] GUO, S., ZHU, H.Y., ZHOU, J., *et al*., "An in situ scanning electron microscope study of void formation induced by typical inclusions in low-density steel during tensile deformation", *Steel Research International*, v. 93, n. 11, pp. 11, Nov. 2022. doi: http://dx.doi.org/10.1002/srin.202200388.

[21] CHU, J., ZHANG, L., YANG, J., *et al*., "Characterization of precipitation, evolution, and growth of MnS inclusions in medium/high manganese steel during solidification process", *Materials Characterization*, v. 194, pp. 112367, 2022. doi: http://dx.doi.org/10.1016/j.matchar.2022.112367.

[22] SU, L.J., TIAN, J., HU, S.Y., *et al*., "Effect of Ca/Mg on distribution and morphology of MnS inclusions in 45MnVS non-quenched and tempered steel", *Metals*, v. 13, n. 1, pp. 16, Jan. 2023.

[23] WANG, Y.L., CHEN, Y.L., WEI, H., *et al*., "Effect of hot rolling process parameters on microstructure transformation and microstructure of 45MnSiV steel", *Materials Science Forum*, v. 944, pp. 265–271, 2019. doi: http://dx.doi.org/10.4028/www.scientific.net/MSF.944.265.

[24] LIU, F., SHEN, N.R., ZHOU, L., *et al*., "Effect of cooling system and forming structure on grain sizes and mechanical properties of S43CMnV for non-quenched and tempered steel crankshaftEinfluss des Kuhlsystems und der Umformungsstruktur auf die Korngrosse und die mechanischen Eigenschaften von S43CMnV fur nicht abgeschreckte und warmebehandelte Stahl-Kurbelwellen", *Materialwissenschaft und Werkstofftechnik*, v. 53, n. 8, pp. 935–946, Aug. 2022. doi: http://dx.doi.org/10.1002/mawe.202100379.